Fingerprint Registration Using Zernike Moments : An Approach for a Supervised Contactless Biometric System

Tahirou DJARA   *csm.djara@gmail.com*
Laboratory of Electronic Engineering,
Telecommunications and Applied data Processing Technology.
Ecole Polytechnique of Abomey Calavi (EPAC).
University of Abomey-Calavi. 01 BP 2009 Cotonou, BENIN.

Marc Kokou ASSOGBA   *mkokouassogba@yahoo.fr*
Laboratory of Electronic Engineering,
Telecommunications and Applied data Processing Technology.
Ecole Polytechnique of Abomey Calavi (EPAC).
University of Abomey-Calavi. 01 BP 2009 Cotonou, BENIN.

Amine NAÏT-ALI   *amine.naitali@gmail.com*
Laboratory Images, Signals and Intelligent Systems
University of Paris Est-Créteil,
122, rue Paul Armangot, 94400 Vitry sur Seine

Antoine VIANOU   *avianou@yahoo.fr*
 Laboratory of Electronic Engineering,
Telecommunications and Applied data Processing Technology.
Ecole Polytechnique of Abomey Calavi (EPAC).
University of Abomey-Calavi. 01 BP 2009 Cotonou, BENIN.

Abstract

In this work, we deal with contactless fingerprint biometrics. More specifically, we are interested in solving the problem of registration by taking into consideration some constraints such as finger rotation and translation. In the proposed method, the registration requires: (1) a segmentation technique to extract streaks, (2) a skeletonization technique to extract the center line streaks and (3) and landmarks extraction technique. The correspondence between the sets of control points, is obtained by calculating the descriptor vector of Zernike moments on a window of size RxR centered at each point. Comparison of correlation coefficients between the descriptor vectors of Zernike moments helps define the corresponding points.   The estimation of parameters of the existing deformation between images is performed using RANSAC algorithm (Random SAmple Consensus) that suppresses wrong matches. Finally, performance evaluation is achieved on a set of fingerprint images where promising results are reported.

Keywords: Contactless Biometry, Fingerprint, Zernike Moments, Image Registration.

1. INTRODUCTION

Due to its unicity, fingerprint is probably one of the most common modality used to identify individuals[1]. However, classical fingerprint devices requiring a direct contact (touch-based) have some main drawbacks related to acquisition conditions such as: eventual elasticity of the finger, environment conditions, hygiene problem (i.e. same sensor touched by users) that can be particularly exacerbated during the outbreak of epidemics or pandemics. To overcome these problems, contactless based-systems seem to be much more appropriate and useful as stated by the US Department of Homeland Security (DHS) which considers that the development of a Biometric Detector prototype capable for acquiring contactless fingerprint for identity

Tahirou DJARA, Marc Kokou ASSOGBA, Amine NAÏT-ALI & Antoine VIANOU

management will improve fingerprint acquisition quality and recognition and reduce false positives [2].

Fingerprint registration is a critical step when dealing with fingerprint matching. The registration is a classic problem in computer vision that occurs in many tasks of analysis and image processing. Every method should take into account not only the assumed type of geometric deformation between the images but also radiometric deformations and noise corruption, required registration accuracy and application-dependent data characteristics [3].

The goal of an algorithm for image registration is to match images 2D or 3D so as to overlay the pixels or voxels representing the same structures. Our method consists in determining the transformation linking the bifurcation points contained in an image to readjust and its correspondence on the other anatomical image (called reference image) as shown in figure 1.
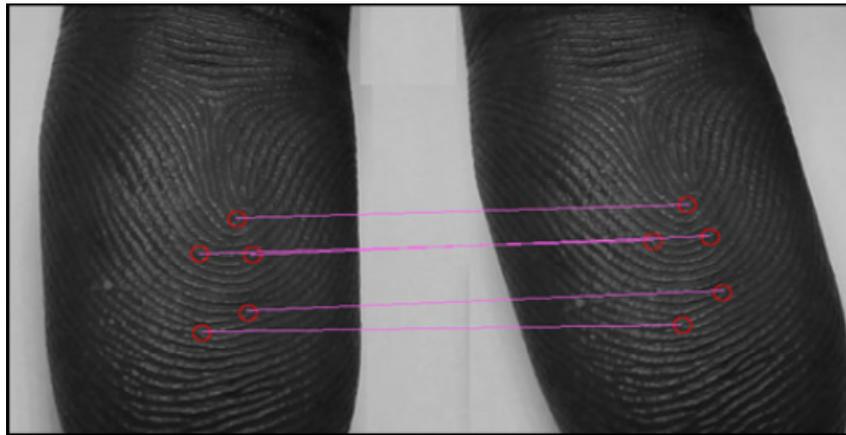
FIGURE 1: Determination of Corresponding Bifurcation.

Although a variety of registration alignment algorithms have been proposed, accurate fingerprint registration remains an unresolved problem [4]. Based on the features that the matching algorithms use, fingerprint matching can be classified into image-based and graph-based matching [5].

Image-based matching [6] uses the entire gray scale fingerprint image as a template to match against input fingerprint images. The primary shortcoming of this method is that matching may be seriously affected by some factors such as image quality variation, and distortion, which are inherent properties of contact fingerprint images.

Graph-based matching [7, 8] represents the minutiae in the form of graphs. The high computational complexity of graph matching hinders its implementation. For instance, in [9] proposed algorithms for matching fingerprints using the relative position of minutiae whose implementation is relatively simple.

In this work, fingerprints are acquired using a simple camera. For registration purpose, we present an approach that deals with minutia for the matching process, combined with techniques developed in [10, 11]. More specifically, we show how one can use Zernike moments for an efficient registration.

This paper is organized as follows: in section 2 we present the experimental condition. The proposed method is presented in section 3. Section 4 contains the discussion about the experimental results, and finally; we conclude our work in section 5.

Tahirou DJARA, Marc Kokou ASSOGBA, Amine NAÏT-ALI & Antoine VIANOU

2. EXPERIMENTAL CONDITIONS

In the literature, there are few studies focused on contactless systems [12, 13]. Most systems require the placement of the finger on predisposed guides in order to simplify the image acquisition step [12, 14]. Experiments are carried out in [12, 15, 16] with different distances and resolution for contactless image acquisition.

2.1 Acquisition Protocol

The contactless fingerprint acquisition system which we are presenting is a part of [12, 14]. We have developed a Contactless Biometric Fingerprint Software (CBFS) for the acquisition and processing our images. It implements our method of fingerprint registration. The contactless fingerprint acquisition system we present consists of this CBFS (Figure 2.b) to visualize the sharpness of the images before capture, a webcam for taking digital photo, and lighting equipment (Figure 2.a). The user is prompted to place the reverse of his finger on a desk. The palm of the user is faced with the webcam. We proceed to the capture of fingerprint. In order to limit travel, a rectangular area is defined on the interface of the webcam which will contain the finger before capture.
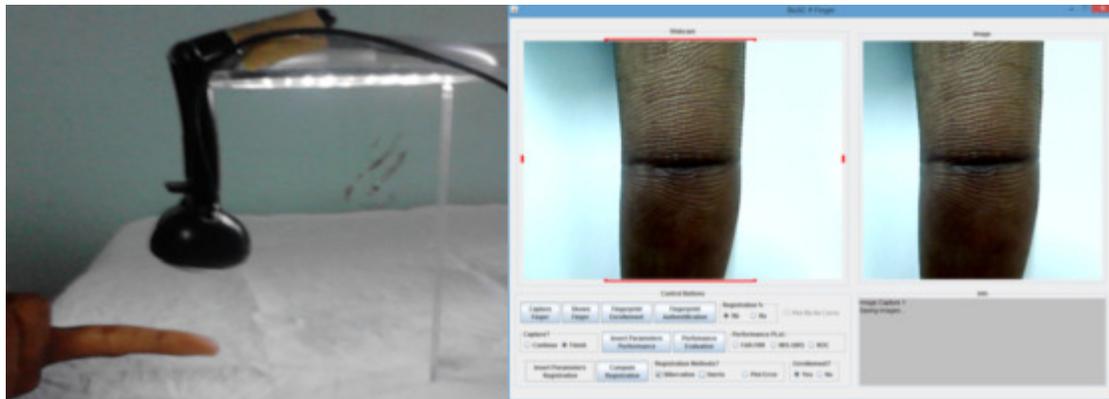
(a)   Acquisition system   (b) The portal of the software

FIGURE 2: Contactless fingerprint acquisition system and Screenshot of CBFS.

2.2 Pre-Processing Phase

The pre-processing phase plays a significant role in improving the image contrast. The contrast enhancement is used to reduce the imperfection which generally occurred due to sensor noise or inconsistent illumination. Histogram equalizing method is used to adjust the distribution of grayscale.

3. PROPOSED METHOD

We have developed a method to proceed with registration of fingerprint images. This registration method aims at determining the $\emptyset = (t_x, t_y, \theta_{xy})^t$ parameters of 2D translation and rotation. Under experimental conditions, our images are obtained at a fixed distance from the sensor, therefore the scale factor is not taken into account.

The proposed registration method is performed in five steps that are detailed as follows:

Step 1. Image segmentation and skeletonization to extract center line (cl) streaks,
Step 2. Automatic selection a set of control points to be matched from the   reference image and the input image,
Step 3. Description of each image using Zernike moments,
Step 4. Definition of a similarity measure to establish a correspondence between the detected corresponding points from the two images,

Step 5. Estimation of parameters that model the best deformation between sets..

3.1 Segmentation
Segmentation is the process of separating foreground regions in an image from background regions. The foreground regions correspond to the clear fingerprint area containing ridges and valleys, which is the area of interest. The background corresponds to the regions outside the borders of the fingerprint area, which do not contain any valid fingerprint information. In our method, we first eliminate the background regions that allow us to obtain an image of the foreground regions (FR). In a second step, the ridges are extracted from FR.

3.1.1. Foreground Regions Extraction
The extraction of streaks is linked to the extraction of foreground regions. For this purpose, we have applied a filter to the image in order to define its contour. Then a binary mask is subsequently applied to the image filter, which allows to have an image defining the contour of the fingerprint. This contour image is used for the extraction of foreground regions.

3.1.2. Streaks Extraction
In order to get the streaks in the image of fingerprint, a photometric adaptive threshold method has been developed [17]. Two thresholds are defined i.e. S_s and S_h corresponding to the mean of a square framework and the mean of a hexagonal framework.

(a) Original Image

(b) Edge detection

(c) Binary mask

(d) Foreground regions
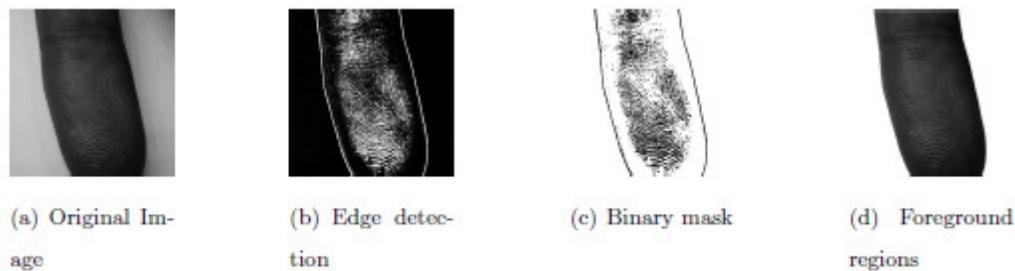
FIGURE 3: Main steps of the extraction of the foreground regions.

A pixel $P(x,y)$ is deleted or not by comparing its value with S_s and S_h. Photometric thresholding being preceded by the extraction of the region of interest. The streaks image is skeletonized in order to get minutiae i.e. streak ending points and streak bifurcation points.

3.2 Automatic Selection of Landmarks
The first step in a process of automatic image registration of fingerprints involves the automatic selection of a set of potential control points from two images F_t and F_{t+d} to realign. The performance at this stage of selection of control points is important because it depicts the quality of registration.

Control points, which should serve as a pivot for distortion correction must be sure points. They must be easily identifiable landmarks and intangible. In [10, 11], an automatic extraction of Landmark-based NSCT (No Sub-sampled Contourlets Transform) has been suggested.

It should be noted that in the case of fingerprint images, the points that naturally characterize them are minutiae. Termination and bifurcation type minutiae are mainly the signature of a fingerprint [18].

We have used the bifurcation points extracted from the algorithm presented in [19] and used in [20] for the detection of minutiae of a fingerprint image.

Tahirou DJARA, Marc Kokou ASSOGBA, Amine NAÏT-ALI & Antoine VIANOU

3.3. Zernike Moments Calculation
3.3.1. Definition and Properties of Zernike Moments
In (ρ, θ) polar coordinates, the Zernike radial polynomials of order p with repetition q are defined by [21]:

$$R_{pq}(\rho) = \sum_{s=0}^{\frac{p-|q|}{2}} \frac{(-1)^s (p-s)!}{s! \left(\frac{p+|q|}{2}-s\right)! \left(\frac{p-|q|}{2}-s\right)!} \rho^{p-2s} \tag{1}$$

In the above equation p is a non-negative integer, (p≥0), and q positive and negative integers subject to the constraints:

$$\begin{cases} p-|q| \ is \ even \\ |q| \le p \end{cases} \tag{2}$$

The Zernike moment of order p with repetition q for a continuous image function $f(x,y)$, that vanishes outside the unit disk is:

$$Z_{pq} = \frac{p+1}{\pi} \iint_{x^2+y^2\le1} V_{pq}^*(\rho,\theta) f(x,y) \, dx \, dy \tag{3}$$

For the digital image, the integrals are replaced by summations [22] to get :

$$Z_{pq} = \frac{p+1}{\pi} \sum_x \sum_y V_{pq}^*(\rho,\theta) F(x,y) \tag{4}$$

with

$$V_{pq}(\rho,\theta) = R_{pq}(\rho) e^{iq\theta} \tag{5}$$

where V_{pq}^* denote complex conjugate of V_{pq}, $\rho = \sqrt{x^2+y^2} \le 1$ and $\theta = tan^{-1}\left(\frac{y}{x}\right)$.

The computation of radial Zernike polynomial $R_{pq}(\rho)$ is performed according to a recursive algorithm [21, 23] by replacing the index $p-2s$ by k in equation (1). We can rewrite the radial polynomials in powers of k as follows :

$$R_{pq}(\rho) = \sum_{k=|q|}^{p} B_{pqk}\rho^k , (p-k \ is \ even) \tag{6}$$

where

$$B_{pqk} = \frac{(-1)^{\frac{p-k}{2}} \left(\frac{p+k}{2}\right)!}{\left(\frac{p-k}{2}\right)! \left(\frac{k+|q|}{2}\right)! \left(\frac{k-|q|}{2}\right)!} \tag{7}$$

Equation (6) is generally preferred to equation (1) for the evaluation of the Zernike polynomials [24]. A study [25] has shown that Zernike moments are less sensitive to noise and less redundant information. Many works like [21, 26] were then performed on the invariance of the moments considering the affine transformation coordinates and intensity changes in grayscale images.

The defined features of Zernike moments themselves are only invariant to rotation. To obtain scale and translation invariance, the image needs to be normalized first by using the regular Zernike moments. Zernike features invariant to translation are then extracted from the normalized image [27].

Tahirou DJARA, Marc Kokou ASSOGBA, Amine NAÏT-ALI & Antoine VIANOU

3.3.2. Zernike Moments on Binary two Fingerprints

Figure 5 shows the Zernike moments computated on binary fingerprint images presented in Figure 4. Image 2 is the $180°$ rotation version of image 2. One can notice that for the two images, we have similar values of Zernike moments. This shows the invariance of Zernike moments in rotation.

(a) Image1   (b) Image 2
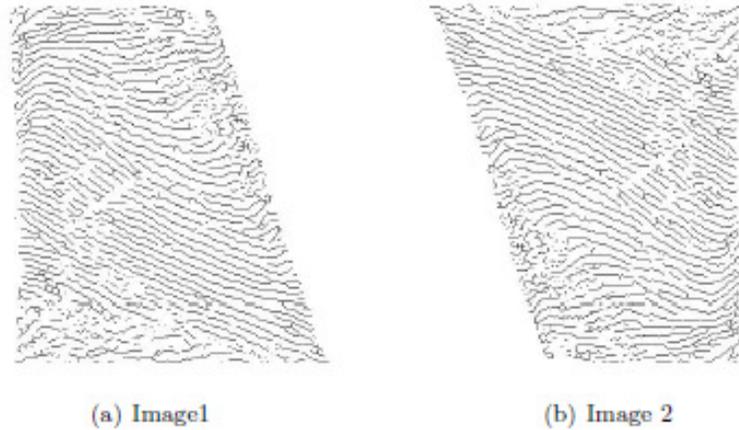
FIGURE 4: Two binary images of fingerprints different of $180°$.

Image1			Image 2 : Image 1 rotated		
pq	$|Z_{pq}|$		pq	$|Z_{pq}|$	
00	0.2893952		00	0.2893952	
11	0.0058495		11	0.0058495	
20	0.1317473		20	0.1317473	
22	0.1051705		22	0.1051705	
31	0.0147638		31	0.0147638	
33	0.0579088		33	0.0579088	
40	0.0547054		40	0.0547054	
42	0.0225529		42	0.0225529	
44	0.0536853		44	0.0536853	
51	0.0009113		51	0.0009113	
53	0.0181444		53	0.0181444	
55	0.0225388		55	0.0225388	

TABLE 1: Module of Zernike moments of two binary fingerprints images different of $180°$.
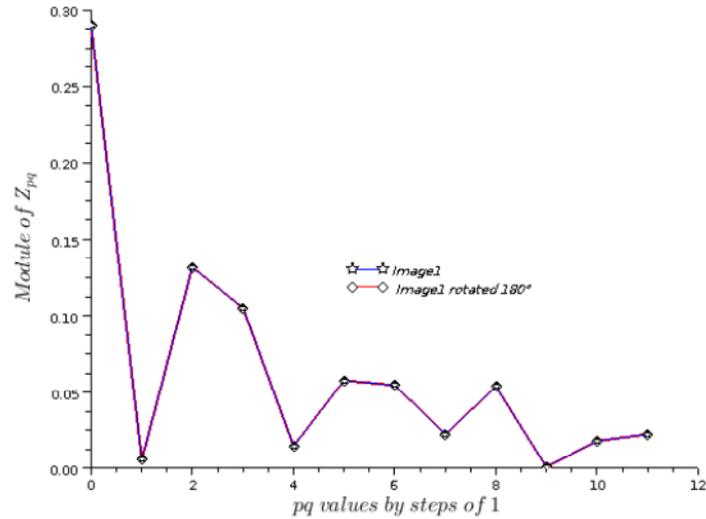
FIGURE 5: Zernike moments applied to the binary image of the Figure 4.

3.4. Matching Process

After extraction of bifurcation points on the cl of realign images to readjust, we are left with two sets of points to match : a set of bifurcation points on the reference image F_t and a set of bifurcation points on the input image F_{t+d}. The correspondence between these two sets of control points is obtained by following steps:

- ✓ Subdivide each image into thumbnail size $L \times L$ centered on each point bifurcations B_i.

- ✓ For each thumbnail centered on this point B_i, construct the descriptor vector of Zernike moments M_z as follows:

$$P_Z = \left(|Z_{11}|, \dots, |Z_{pq}|, \dots, |Z_{55}| \right) \tag{8}$$

where $|Z_{pq}|$ is the module of Zernike moments. We have used as the highest order of moments 5 after several experimental trials. Although the higher order moments are the fine details of the image, they are more sensitive to noise than lower order moments.

- ✓ For any point r_i of the reference image, we suppose that its corresponding e_i of input image is from a set of points on F_{t+d}. located within a certain radius R' around r_i. The radius R' limits the search for corresponding and therefore, reduces the number of comparisons to achieve in order to find out the corresponding points.
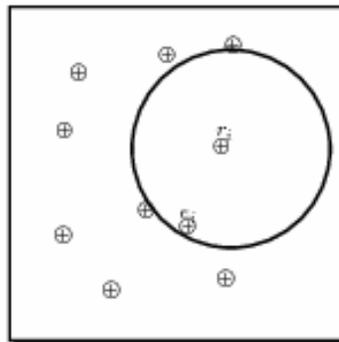
FIGURE 6: Determining the corresponding e_i (of input image F_{t+d}) of a bifurcation point r_i (of the reference image F_t).

- ✓ The matching process is performed by calculating the correlation coefficients between the two vectors descriptors. The corresponding points are those which give the maximum value of correlation coefficient.

The correlation coefficient between two vectors of the feature $X(x_1, \dots, x_n)$ and $Y(y_1, \dots, y_n)$ is given by the following formula:

$$C = \frac{\sum_{i=1}^{n}(x_i - \bar{x}) \cdot (y_i - \bar{y})}{\sqrt{\sum_{i=1}^{n}(x_i - \bar{x})^2} \cdot \sqrt{\sum_{i=1}^{n}(y_i - \bar{y})^2}} \tag{9}$$

where $\bar{x}$ and $\bar{y}$ are averages of the two vectors X and Y respectively.
If C is 0, the two vectors are not correlated. The two vectors are even better correlated than C is far from 0 (near -1 or 1).

3.5. Estimation of the Registration Geometric Transformation
Once the information type to be used to guide the registration and the similarity criterion quantifying the similarity between two images are defined, the model of deformation is determined to realign the images. The choice of the model of deformation is very important and is guided by the underlying application and the information, at first instant, available about the nature of the deformation between the images.

The geometric transformations or deformation models involved in the registration of 2D images are generally of rigid, affine or curvilinear [28].

3.5.1. Rigid Transformation
A registration transformation is rigid when it conserves the distance between any two points. Only the rotation and translation are taken into account. Coordinates (x, y) of any point M of the image to readjust are transformed as follows :

$$\begin{pmatrix} x' - x_0 \\ y' - y_0 \end{pmatrix} = \begin{pmatrix} cos\theta & -sin\theta \\ sin\theta & cos\theta \end{pmatrix} \begin{pmatrix} x - x_0 \\ y - y_0 \end{pmatrix} + \begin{pmatrix} t_x \\ t_y \end{pmatrix} \tag{10}$$

where $M_0 \begin{pmatrix} x_0 \\ y_0 \end{pmatrix}$ is the center of rotation, θ the angle of rotation, $\begin{pmatrix} t_x \\ t_y \end{pmatrix}$ the coordinates of the translation vector and $M' \begin{pmatrix} x' \\ y' \end{pmatrix}$, the transform of M.

3.5.2. Affine Transformation
A registration transformation is affine when it preserves parallelism and takes into account the difference in scale between the images. The coordinates $\begin{pmatrix} x \\ y \end{pmatrix}$ of any point of the image to readjust are transformed as follows :

$$\begin{pmatrix} x' \\ y' \end{pmatrix} = \begin{pmatrix} a_{11} & a_{12} \\ a_{21} & a_{22} \end{pmatrix} \begin{pmatrix} x \\ y \end{pmatrix} + \begin{pmatrix} t_x \\ t_y \end{pmatrix} \tag{11}$$

with $a_{11}, a_{12}, a_{21}, a_{22}$ real coefficients and $\begin{pmatrix} t_x \\ t_y \end{pmatrix}$ the translation vector coordinates.

3.5.3. Curvilinear Transformation
A registration transformation of the curvilinear type is a polynomial function. It takes into account the distortions between the images. The coordinates $\begin{pmatrix} x \\ y \end{pmatrix}$ of any point of the image to readjust are transformed as follows :

$$\begin{cases} x' = a_{00} + a_{10}x + a_{01}y + a_{20}x^2 + a_{11}xy + a_{02}y^2 + \cdots \\ y' = b_{00} + b_{10}x + b_{01}y + b_{20}x^2 + b_{11}xy + b_{02}y^2 + \cdots \end{cases} \quad (12)$$

with a_{ij} , b_{ij}, real coefficients.

Figure 7 shows a practical example of the different transformations.

(a)   (b)

(c)   (d)
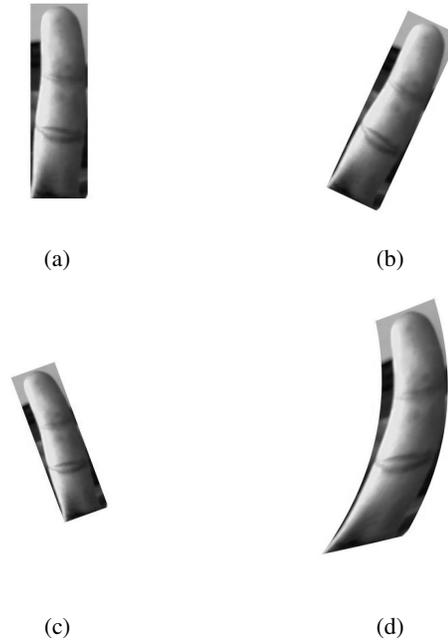
FIGURE 7: Practical examples of different types of registration geometric transformation. (a) Input image, (b) Rigid transformation, (c) Affine transformation, (d) Curvilinear transformation.

3.5.4. Deformation Model Retained
The transformation model used to produce the image distortion F_{t+d} is the rigid transformation model expressed by Equation (10). This model is appropriate for the case of our fingerprint images captured at a fixed distance from the sensor.

The estimation of the parameters of the rigid transformation is carried out iteratively. At each iteration we provide online processing parameters found by RANSAC.

The RANdom SAmple Consensus (RANSAC) is an algorithm proposed for the first time in 1981 by Fischler and Bolles [29]. It is a general parameter estimation approach designed to cope with a large proportion of outliers in the input data. This is a popular method in regression problems containing aberrant data or outliers [30].

As pointed out by Fischler and Bolles [29], unlike conventional sampling techniques that use as much of the data as possible to obtain an initial solution and then proceed to prune outliers, RANSAC uses the smallest set possible and proceeds to enlarge this set with consistent data points [29]. In [31, 32], RANSAC is used to refine the search for matching between the pores in the fingerprint identification process of individuals.

Tahirou DJARA, Marc Kokou ASSOGBA, Amine NAÏT-ALI & Antoine VIANOU

The basic RANSAC algorithm is summarized as follows :

Algorithm 1 RANSAC

1: Select randomly the minimum number of points required to determine the model parameters.
2: Solve for the parameters of the model.
3: Determine how many points from the set of all points fit with a predefined tolerance ϵ.
4: If the fraction of the number of inliers over the total number points in the set exceeds a predefined threshold τ, re-estimate the model parameters using all the identified inliers and terminate.
5: Otherwise, repeat steps 1 through 4 (maximum of N times).

The number of iterations, k, is chosen high enough to ensure that the probability p (usually set to 0.99) that at least one of the sets of random samples does not include an outlier. Let w represent the probability that any selected data point is an inlier and $\varepsilon = 1 - w$ the probability of observing an outlier.

A common case is that w is not known in advance, but an approximate value can be estimated using the following algorithm [33].

Algorithm 2 : Adaptive algorithm for determining the number of RANSAC samples[33].
Require: $k = \infty$, $sample\,count = 0$.

1: **while** $k > sample\,count$ **do**
2:      Choose a sample and count the number of inliers
3:      Set $\varepsilon = 1 - \dfrac{number\,of\,inliers}{total\,number\,of\,points}$
4:      Set k from ε and (13) with $p = 0.99$
5:      Increment the sample count by 1
6: **end while**

According to [33, 34], the maximum number of iterations of the algorithm is given by :

$$k = \frac{\log(1-p)}{\log(1-(1-\varepsilon)^n)} \qquad (13)$$

where n is the size of the sample.

Figure 8, shows an example of 7 pairs of points of interest including 3 red discharged after treatment of the RANSAC algorithm.
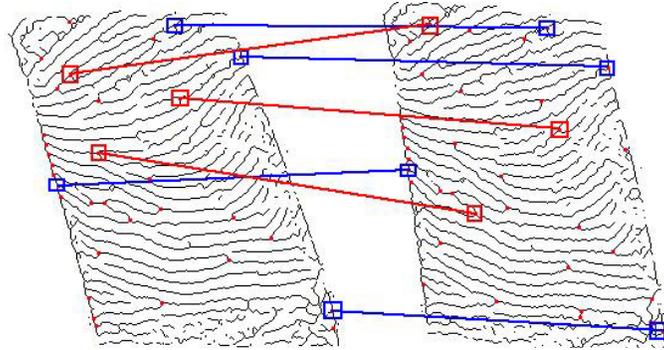
FIGURE 8: 7 pairs of correspondents found in the matching process including 3 red rejected by RANSANC.

4. Experimental Results

This section is dedicated to the validation and the evaluation of the performances of the proposed registration algorithm in terms of precision.

In order to evaluate the precision of the proposed registration algorithm, we have used a first time synthetic geometric distortion. The deformation model chosen was applied to a database of fingerprint images that we have formed. Our test image database consists of 80 grayscale images of size 480×480 pixels. Ten images are shown in Figure 9. In a second phase, we used images acquired at different times, so deformation is not known in advance. We have applied the different stages of the registration to these images.

(a)	(b)	(c)	(d)	(e)	(f)	(g)
(h)	(i)	(j)				
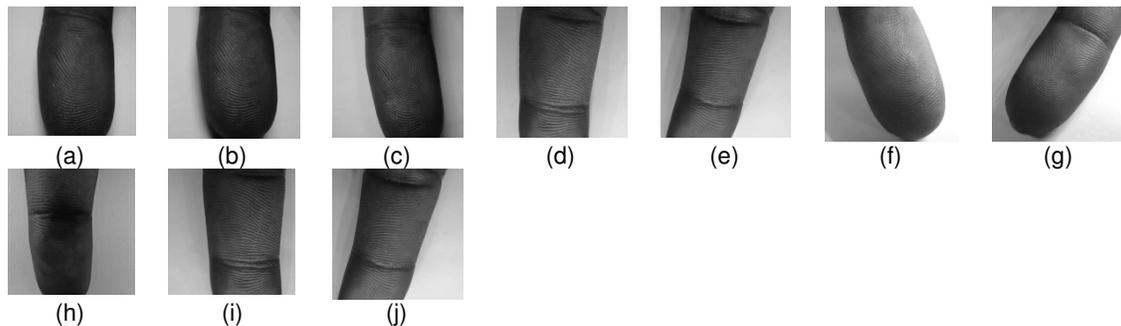
FIGURE 9: 10 images of 80 images contained in our database.

The registration method developed is based on the calculated Zernike moments in each point of interest. In the research phase of points, the introduction of the parameter limiting the search area has significantly made it possible to reduce the running time of finding a correspondent from 1106ms to 93ms.

We have written a Java code, implemented through the CBFS in order to implement the proposed method.

The first test can be described in the following steps:

1. Rotation(R) and Translation(T) transformations have been applied to the test images(I). We used the Random Java function to generate randomly for each image vector of translation and rotation. $R \in [1; 19]$ and $T \in \langle (3; 3) \ldots (9; 9) \rangle$.

2. Performance analysis of the algorithm : To plot the curve of the actual parameters and the curve of the estimated parameters to show the accuracy of the algorithm.

Tahirou DJARA, Marc Kokou ASSOGBA, Amine NAÏT-ALI & Antoine VIANOU

3. Computation of error between each real parameters and its estimated parameters, using the following equation:

$$\varepsilon_i = \frac{|\theta_i - \theta_i'|}{\theta_i} \qquad (14)$$

where ε_i is the error associated with estimating angles.

The second test is to work with two images acquired at different times thus deformation unknown. The test consists of following steps:

1. Estimate of the existing deformation between the two images.

2. Quantification of the precision of the estimated transformation. Here, we have measured the precision by the Root Mean Square Error (RMSE), which represents the distance between the position of a control point, once the image, is corrected, and its position on the reference image. It is given by the following formula:

$$RMSE = \sqrt{\frac{1}{M}\left(\sum_i \left\|(x_i, y_i) - T_{affine}^{-1}(x'_i, y_i')\right\|^2\right)} \qquad (15)$$

where (x'_i, y_i') is the correspondent of (x_i, y_i) control point of the reference image, T_{affine} is the estimated affine transformation, $\left\|(x_i, y_i) - T_{affine}^{-1}(x'_i, y_i')\right\|$ is the euclidean distance and M is the number of interest pairs points.

Figure 10 shows the representation of real and estimated orientations of test images based on the hyperbolic cosine function:

$$f : \theta \mapsto \cosh(\theta) = \frac{e^\theta - e^{-\theta}}{2} \qquad (16)$$
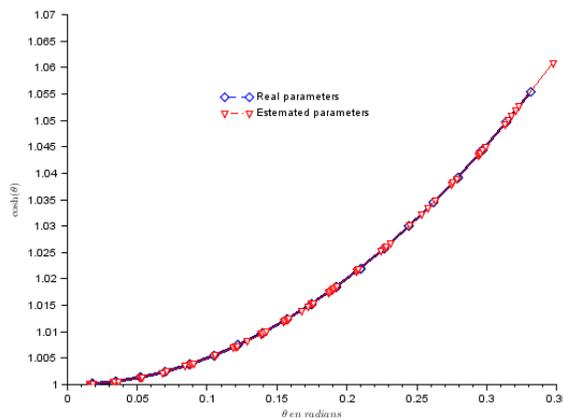
FIGURE 10: Real parameters and estimated parameters.
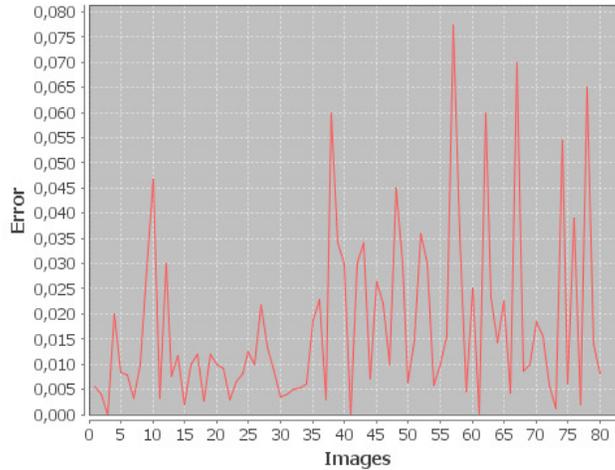
FIGURE 11: Error between original images and transformed images.

It may be noted that we have similar values between the estimated orientation and the real orientation for each image. This is confirmed by the Figure 11 which represents the relative error between the two parameters. The largest error is less than 0.08, while the smallest is about 0.

For the first test, we only show in a Figure 12 the results obtained by the proposed method in image of Figure 9-(a). The Figure 12-(d), show the result of the registration of the images in grayscale, while the Figure 12-(f) show the result of the registration lc extracted from the images in Figure12-(a)-(b). Figure 13 shows the zoom of the framed images of Figure 12-e and 12-f.

(a) Reference image (b) Distorted version of (a) (c) Superposition of (a) and (b) before registration (d) Superposition of (a) and (b) after registration (e) Superposition of center lines before registration (f) Superposition of center lines after registration
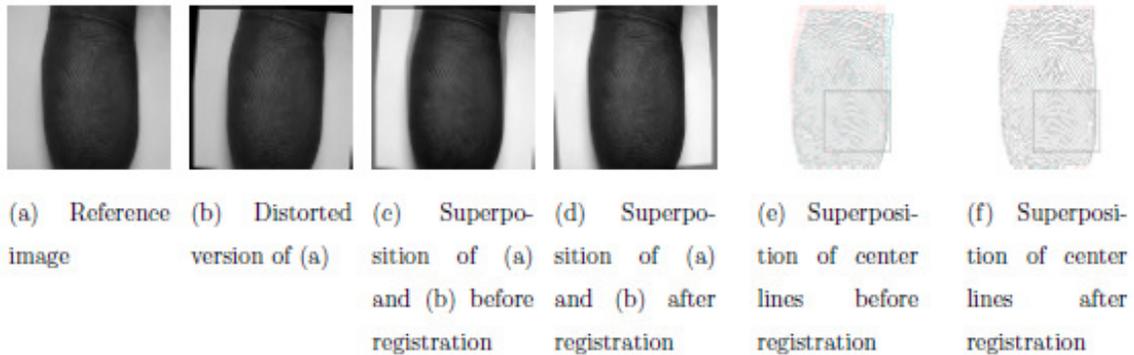
FIGURE 12: Result of registration. The image (a) has undergone a rotation angle of $\theta = 4°$ and a translation vector $\vec{T} = (10 pixels, 5 pixels)$.

(a) Zoom a zone of (e) (b) Zoom a zone of (f)
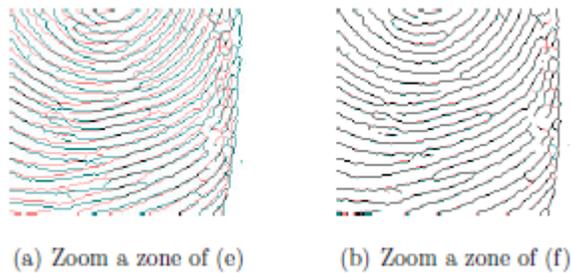
FIGURE 13: Zoom framed parts of the lc (e) and (f).

Tahirou DJARA, Marc Kokou ASSOGBA, Amine NAÏT-ALI & Antoine VIANOU

On the second test, we show the results obtained by the proposed method in image of Figure 14. The Figure 14-(d), shows the result of the registration of the images in grayscale, while the Figure 14-(f) shows the result of the registration lc extracted from the images in Figure 14-(a)-(b). Figure 15 shows the zoom of the framed images of Figure 14-(e) and 14-(f).

(a) Reference image (b) Secondary image (c) Superpo-sition of (a) and (b) before registration (d) Superpo-sition of (a) and (b) after registration (e) Superposi-tion of center lines before registration (f) Superposi-tion of center lines after registration
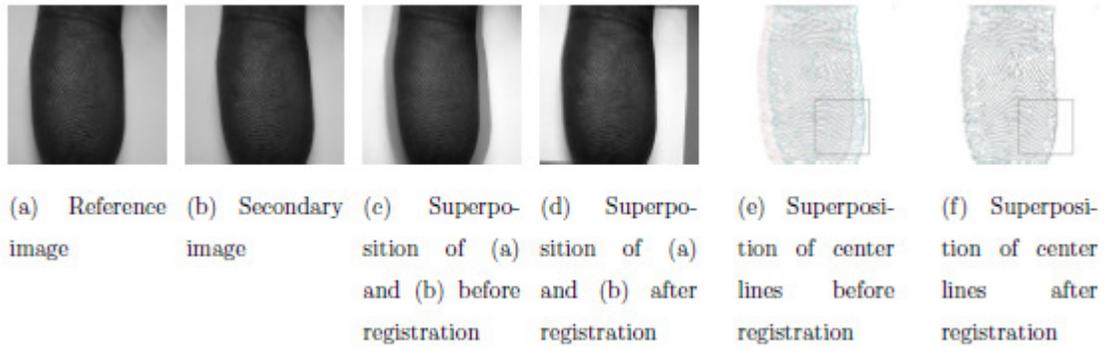
FIGURE 14: Result of registration. The images (a) and (b) are acquired at different times.

(a) Zoom a zone of (e)   (b) Zoom a zone of (f)
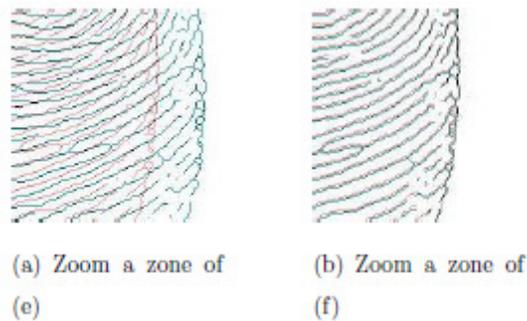
FIGURE 15: Zoom framed parts of the lc (e) and (f).

The results in Table 4, show that on each interest point, landmark error is less than 1 pixel. The value of the RMSE calculated on the total 13 points is less than 0.5 pixel, which is relatively high precision.

Interest points	1	2	3	4	5	6	7	8
RMSE	0.5660	0.1608	0.4171	0.0270	0.0287	0.0020	0.36894	0.1985

Interest points	9	10	11	12	13	RMSE totale
RMSE	0.0593	0.0435	0.0965	0.0874	0.2004	0.4166

TABLE 2: Second test : The RMSEs calculated at interest points (in pixels).

We compared our method to that used descriptors Scale Invariant FeatureTransform [35]. A plugin implements a registration method SIFT operator ImageJ was developed under the name of "SIFT Correspondences Extract" and "Extract MOPS Correspondences". We built this plugin to our platform to conduct experiments. The plugins "Extract SIFT Correspondences" and "Extract MOPS Correspondences" identify a set of corresponding points of interest in two images and export them as PointRoi. Interest points are detected using the Difference of Gaussian detector thus providing similarity-invariance [36]. Corresponding points are best matches from local feature descriptors that are consistent with respect to a common geometric transformation. The plugins use the Scale Invariant Feature Transform (SIFT) and Multi-Scale Oriented Patches (MOPS) for local feature description. The thus established matches are filtered using the RANSAC.

Figure 16 gives an illustration of the error curve for both methods with respect to the estimate of the rotation angle. The minimum error for both methods is 0 while the maximum error is 0.08 for our method and 0.043 for the method using SIFT.
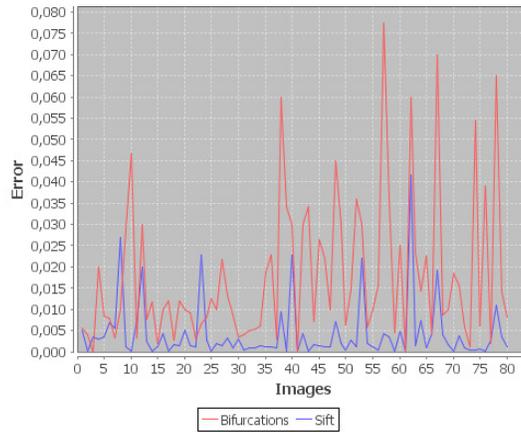
FIGURE 16: Relative error curves.

For the estimation of the translation vector, we have represented the module of real translation vectors and module of estimated translations vectors by each method. Figure 17 shows that the two modules regarding the real translations vectors and those estimated by our method are nearby. It may be noted at Figure 18 there is a very poor estimate of translation vectors by the method using SIFT.
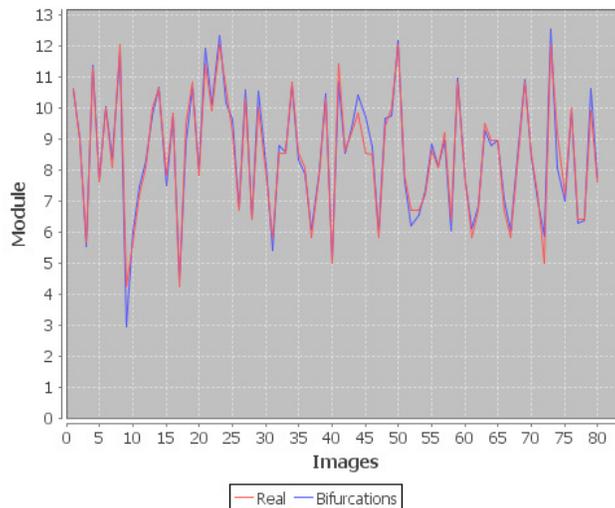
FIGURE 17: Module parameters real and estimated by bifurcations.
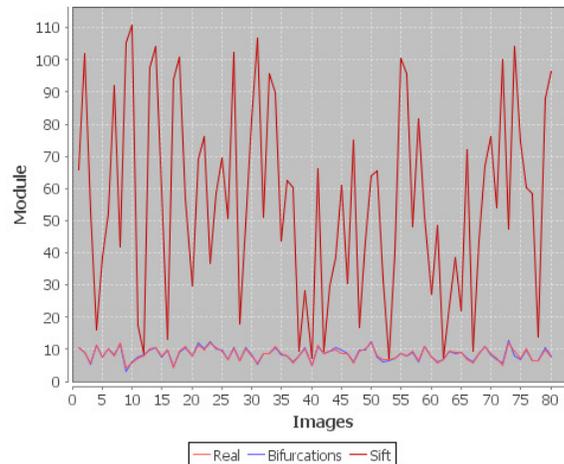
FIGURE 18: Module parameters real and estimated by bifurcations and SIFT.

5. CONCLUSION

In this paper, we have presented a new approach of the registration of fingerprint images that includes a segmentation technique to extract the streaks, a skeletonization technique to extract the center line streaks and a technique for extracting landmarks to guide the registration. The corresponding points, enabling the quantification of the deformation parameters existing between the images are obtained by comparing the correlation coefficients between the descriptor vectors of Zernike moments. The results obtained have allowed us to measure the reliability of the proposed method. The remaining work is about individuals identification using our registration method.

6. REFERENCES

[1] S. Pankanti, S. Prabhakar, A. Jain, On the individuality of fingerprints, IEEE Trans. Pattern Anal. 24 (8) (2002) 1010–1025.

[2] Biometric in governements post-9/11, National Science and Technology Council, http://www.biometrics.gov/Documents/ (2009) 71–73, [Oct. 20, 2014].

[3] B. Zitova, J. Flusser, Image registration methods: a survey, Image and Vision Computing 21 (2003) 977–1000.

[4] L. Liu, T. Jiang, J. Yang, al, Fingerprint registration by maximization of mutual information, IEEE Transactions on image processing 15 (5) (2006) 1100–1110.

[5] K. Mali, S. Bhattacharya, Fingerprint recognition using global and local structures, International Journal on Computer Science and Engineering (IJCSE) 3 (1) (2011) 161–172.

[6] R. Bahuguna, Fingerprint verification using hologram matched filterings, Psychological Review Presented at the 8th Meeting Biometric Consortium, San Jose, CA, Jun. 1996.

[7] S. Gold, A. Rangarajan, A graduated assignment algorithm for graph matching, IEEE Trans. Pattern Anal. 18 (4) (1996) 377–388.

[8] D. K. Isenor, S. G. Zaky, Fingerprint identification using graph matching, Pattern Recognit. 19 (2) (1986) 113–122.

[9] Y. He, J. Tian, X. Luo, T. Zhang, Image enhancement and minutiae matching in

fingerprint verification, Pattern Recognition Letters 24 (2003) 1349–1360.

[10] C. Serief, Robust feature points extraction for image registration based on the nonsubsampled contourlet transform., International Journal of Electronics Communication. 63 (2) (2009) 148–152.

[11] J. Sarvaiya, S. Patnaik, H. Goklani, Image registration using nsct and invariant moment, International Journal of Image Processing (IJIP) 4 (2) (2010) 119–130.

[12] G. Parziale, E.-D. Santana, R. Hauke, The surround imager: A multi-camera touchless device to acquire 3d rolled-equivalent fingerprints, ICB, LNCS 3832 (2006) 244–250.

[13] B. Hiew, A. Teoh, Y. Pang, Touch-less fingerprint recognition system, ICB, LNCS 3832 (2007) 24–29.

[14] S. Mil'shtein, J. Palma, C. Liessner, M. Baier, A. Pillai, A. Shendye, Line scanner for biometric applications, IEEE Intern. Conf. on Technologies for Homeland Security (2008) 205–208.

[15] R. D. Labati, A. Genovese, V. Piuri, F. Scotti, Measurement of the principal singular point in contact and contactless fingerprint images by using computational intelligence techniques, IEEE International Conference on Computational Intelligence for Measurement Systems and Applications (CIMSA) (2010) 18–23.

[16] C. Lee, S. Lee, J. Kim, S. J. Kim, Preprocessing of a fingerprint image captured with a mobile camera, ICB, LNCS 3832 (2006) 348–355.

[17] T. Djara, M. K. Assogba, A. Naït-Ali, Caractérisation spatiale des empreintes de l'index en analyse biométrique, Actes du CARI, Yamoussoukro (2010) 501–508.

[18] W. Osterburg, T. Parthasarathy, T. E. S. Raghavan, al, Developpement of a mathematical formula forthe calculation of fingerprint probabilities based on individual characteristics, Journal of the American Statistical Association 72 (360) (1977) 772–778.

[19] C. Arcelli, G. S. di Baja, A width-independent fast thinning algorithm, IEEE Trans. Pattern Anal. Mach. Intell. (1985) 463–474.

[20] N. Galy, Etude d'un système complet de reconnaissance d'empreintes digitales pour un capteur microsystème à balayage, Institut National Polytechnique de Grenoble - INPG (Thèse) (2005) 463–474.

[21] R. J. Prokop, A. P. Reeves, A survey of moment-based techniques for unoccluded object representation and recognition, Computer Vision, Graphics, and Image Processing. Graphical Models and Image Processing 54 (5) (1992) 438–460.

[22] R. Mukundan, K. R. Ramakrishnan, Moment Functions in Images Analysis. Theory and Applications, (1998), Ch. Zernike Moments, pp. 57–68.

[23] R. Mukundan, K. R. Ramakrishnan, Fast computation of Legendre and Zernike moments, Pattern Recognition 28 (9) (1995) 1433–1442.

[24] R. Mukundan, A contour integration method for the computation of zernike moments of a binary image, National Conference on Research and Development in Computer Science and its Applications (1997) 188–192.

[25] W. Y. Kim, P. Yuan, A practical pattern recognition system for translation, scale, and rotation invariance, In Proceedings of the Conference on Computer Vision and Pattern Recognition, IEEE Computer Society Press (1994) 391–396.

[26] L. V. Gool, T. Moons, D. Ungureanu, Affine/photometric invariants for planar intensity patterns, In Proceedings of the 4th European Conference on Computer Vision (1996) 642–651.

[27] A. Khotanzad, Y. H. Hong, Invariant image recognition by zernike moments, IEEE Trans. Pattern Anal. Mach. Intell. 12 (5) (1990) 489–497.

[28] P. A. Elsen, E. J. D. Pol, M. A. Viergever, Medical image matching a review with classification, IEEE Engineering in Medecine and Biology (1993) 26–39.

[29] M. A. Fischler, R. C. Bolles, Random sample consensus: A paradigm for model fitting with applications to image analysis and automated cartography, Communications of the ACM, 24(6) (1981) 381–395.

[30] T. Kim, W. Yu, Performance evaluation of ransac family, In Proceedings of the British Machine Vision Conference (BMVC). (2009) 1–12.

[31] Q. Zhao, L. Zhang, D. Zhang, N. Luo, Direct pore matching for fingerprint recognition, M. Tistarelli and M.S. Nixon (Eds.), ICB (2009) 597–606.

[32] F. Liu, Q. Zhao, L. Zhang, D. Zhang, Fingerprint pore matching based on sparse representation, Pattern Recognition (ICPR) (2010) 1630–1633.

[33] R. Hartley, A. Zisserman, Multiple View Geometry in Computer Vision, 2nd Edition, (2004), Ch. Estimation - 2D Projective Transformations, pp. 117–121.

[34] T. Svoboda, Ransac random sample consensus, http://cmp.felk.cvut.cz (2008) 1–18.

[35] Lowe, David G. "Distinctive Image Features from Scale-Invariant Keypoints". *International Journal of Computer Vision* **60** (2): 91–110. (2004).. doi:10.1023/B:VISI.0000029664.99615.94.

[36] Stephan Saalfeld. "Feature Extraction SIFT/MOPS (Fiji)". (2008). http://fiji.sc/Feature_Extraction